Biomed Eng Lett (2011) 1:70-81
DOI 10.1007/s13534-011-0019-6

REVIEW ARTICLE

Positron Emission Tomography (PET) Detectors with Depth-of-Interaction (DOI) Capability

Mikiko Ito, Seong Jong Hong and Jae Sung Lee

Received: 7 May 2011 / Accepted: 16 May 2011

Abstract
Because positron emission tomography (PET) provides biochemical information in vivo with the sensitivity at the sub-pico-molar level, pre-clinical research using PET plays an important role in biological and pharmaceutical sciences. However, small animal imaging by PET has been challenging with respect to spatial resolution and sensitivity due to the small volume of the imaging objects.
A DOI-encoding technique allows for pre-clinical PET to simultaneously achieve high spatial resolution and high sensitivity. Thus many DOI-encoding methods have been proposed. In this paper we describe why DOI measurements are important, what is required in DOI-encoding designs, and how to extract DOI information in scintillator-based DOI detectors.
Recently, there has been a growing interest in DOI measurements for TOF PET detectors to correct time walk as a function of DOI position. Thus, the DOI-encoding method with a high time performance suitable for TOF detectors is now required. The requirements to improve the time resolution in DOI detectors are discussed as well.

Mikiko Ito, Jae Sung Lee (✉)
Department of Nuclear Medicine, Seoul National University College of Medicine 28 Yungun-Dong, Chongno-Gu, Seoul 110-744, Korea
Tel : +82-2-2072-2938 / Fax : +82-2-745-2938
E-mail : jaes@snu.ac.kr

Seong Jong Hong
Department of Radiological Science, Eulji University, Gyeonggi-do, Korea

Jae Sung Lee
Departments of WCU Brain & Cognitive Sciences and Biomedical Sciences, Seoul National University, Seoul, Korea

Mikiko Ito, Jae Sung Lee
Institute of Radiation Medicine, Medical Research Center, Seoul National University, Seoul, Korea

Keywords Positron emission tomography (PET), Depth of interaction (DOI), Multi-layer detector, Dual-ended readout, Single-ended readout

THE IMPORTANCE OF DOI MEASUREMENT

Simultaneous improvement in spatial resolution and sensitivity

The PET is an important pre-clinical imaging technique because PET provides biochemical information down to the sub-pico-molar level in vivo [1]. Thus, the development of pre-clinical PET scanners has been actively promoted. The major focus of the development is to obtain a similar quality in small animal images as human images, while the size of the imaging subject decreases and the amount of radiopharmaceutical injected into the small animals is limited [2].

To obtain a similar level of detail and SNR in mouse images as human images, spatial resolution and sensitivity should be increased. That is why many PET instrument researchers have been attempting for the pre-clinical PET to simultaneously achieve high spatial resolution and high sensitivity. The pre-clinical PET systems therefore have been designed by using very long and narrow crystals with small diameter ring geometry.

However, such system structures cause the parallax error to become lager when providing no depth-of-interaction (DOI) information within crystals (general PETs can measure no DOI information), and bring the degradation of the radial resolution in the peripheral field of view (FOV). That is because the reconstruction algorithm, when drawing a line of response (LOR) without DOI information, usually assigns the interaction positions over all depths within a crystal to a single position (i.e. the center position on the front of the interacted crystals). The single-positioning method causes

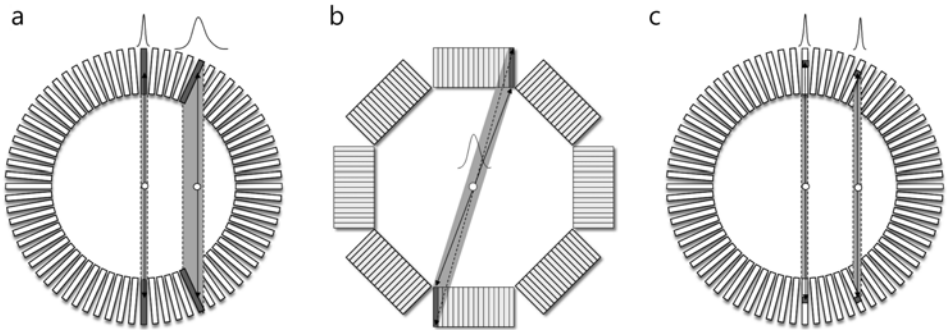

Fig. 1. Effect of parallax error correction by DOI information in peripheral FOV of small-ring PET systems. (a) parallax error at the corner of FOV in PET ring geometry, (b) parallax error at the center of FOV in polygonal PET systems, and (c) reduction of parallax error by DOI information.

the mis-positioning of LOR, referred to as parallax error, due to the penetration of obliquely incidence gamma rays emitted from peripheral FOV, as illustrated in Fig. 1a [3, 4]. Spatial resolution is degraded due to the parallax error as the distance from the center of the FOV increases in the radial direction [5, 6]. In addition, the parallax error can affect the resolution at the center of the FOV if the PET detectors are constructed using a flat panel PMT that has a large entrance window, such as a Hamamatsu H8500 or H9500 because the gamma rays from the center of the FOV obliquely enter into the crystals at the corner of the detectors, as illustrated in Fig. 1b.

On the other hand, if the DOI information is known, the parallax error can be eliminated, as shown in Fig. 1c [7]. Consequently, DOI-encoding PET detectors allow small ring scanners with long crystals to have uniform spatial resolution in all directions without the degradation due to the parallax error [8]. In the case of flat panel PET scanners, DOI information enhances the spatial resolution, even at the center of the FOV.

Time work correction

Recently, there has been an increasing interest in DOI measurement in time-of-flight (TOF) PET detectors to correct the time walk as a function of DOI positions inside the crystals because DOI information can observe the timing error arising in the scintillation crystals due to a propagation speed difference between annihilation radiation and scintillation photons [9]. Thus, DOI information brings TOF PETs to improve timing accuracy. Still, the effect of DOI in TOF has not been extensively studied due to the fact that the current time resolutions of TOF PET are not precise enough for the DOI to have a considerable effect [10].

However, as improvement in time resolution significantly progresses (~100 ps), DOI correction becomes a prominent factor for the TOF detector to improve time resolution. In addition, the TOF resolution in the near future is expected to improve SNR, even for small volume objects such as the brain and breast; the dedicated-specific organ PETs, such as breast and brain PETs, have been actively developed with DOI-encoding detectors that allow small-ring structures with a high fraction of useful FOV of the scanners (the structures close to the patient lead to a higher sensitivity). In addition, TOF information allows the limited angle PET system structures for biopsy [11]; especially in the case of breast cancer evaluation, a needle biopsy may still be necessary to determine tumor cells.

Therefore, a DOI encoding technique would be now required, even for the specific organ or whole body PET scanners as well as pre-clinical PETs when combined with TOF PET detectors.

REQUIREMENTS FOR DOI-ENCODING PET DETECTORS

Because the DOI measurement basically aims to improve PET image quality, the ideal DOI-encoding detector should provide good DOI information without any degradation of other performances in PET scanners, particularly spatial resolution, sensitivity, and energy resolution. Therefore the ideal DOI-encoding detector should have the basic requirements to achieve high performance in PET scanners.

At the level of the detector, excellent 3D positioning ability for gamma ray interaction within crystals is required to achieve high spatial resolution in reconstructed images.

The sensitivity of the system is determined by the event-detection efficiency of the detector in the system and the covered solid angle by the detectors. For high efficiency, the detector should utilize thick crystal block constructed by dense crystals with large packing fraction structure. The detector structure should be suitable to build a full-ring system with minimum gap between the detectors for the large solid angle covered by the detectors. The electronics should have a short dead time which is sufficient to deal with all detected counts.

Selecting the true coincidence events is also important to improve image quality because scattered and random events deteriorate spatial resolution and image contrast. Then, high energy resolution helps distinguish and reject the scattered events. Good time resolution that allows a prompter time window can reduce the random events.

On the other hand, time resolution has been regarded not to be important in the pre-clinical imaging because random rates are generally low and there is no current expectation of obtaining TOF resolution (~600 ns) sufficiently low to be useful for such small volumes [12]. Thus, most proposed DOI-encoding designs were designed without consideration of time performance. However, a new DOI-encoding design with excellent time performance is now required to integrate into the TOF technique. The issue for the manufacturing cost of DOI-encoding designs is being magnified, especially for TOF-DOI detectors employed in specific-organ or whole-body PET scanners constructed with larger ring diameters involving more detectors than pre-clinical PETs. Nevertheless, most DOI-encoding designs bring the escalating cost by the increase in the number of crystals, photosensors, or output channels to deal in electronics. When considering the commercial feasibility, it is important to reduce the manufacturing cost and complication in the electronics. Accordingly, the requirements to be impressive DOI-encoding PET detectors in the future are as follows:

- Good DOI resolution (continuous DOI information)
- Good crystal identification (good intrinsic resolution)
- High stopping power (high packing fraction + thick scintillation crystal block)
- Detector structure able to build a full-ring system with minimum gap between the detectors
- Short dead time
- Good energy resolution
- Good time resolution (for TOF-DOI detectors)
- Low manufacturing cost

Requirements for high timing resolution

Time resolution is influenced by many factors, including the DOI identification, light transport, light collection, detector design, and characteristics of the photosensors [13, 14]. First, as above-mentioned, DOI information can correct a difference in the transport time between events with different DOI positions.

Second, light transport is related to the light collection efficiency and the arrival time dispersion of individual scintillation photons on photosensors that directly influence the time resolution. The light transport is affected by the crystal geometric shape, crystal surface treatment, and detector design. The geometric shape of scintillation crystals should be optimized to reduce the path length between the origin of the scintillation light and the photosensor, and also maximizes the light collection efficiency [15]. The long path length and multiple reflections cause light collection loss and arrival time dispersion of scintillation light, and degrade time performance. For long crystals, the surface treatment of the scintillation crystal is preferred to be polished than "as cut" or rough (diffuse) surface for high light collection efficiency. The "as cut" surface cause light collection loss along the DOI position due to diffuse reflection that makes the light path length increased. In contrast, the polished surface maintains uniform light collection efficiency against DOI position [16, 10]. The light collection loss along DOI positions deteriorates the time resolution because the time resolution is inversely proportional to the square root of the number of photo-electrons per pulse [17, 18]. For detector module design, it is advanced that individual crystals are coupled one-to-one to photosensors directly instead of the use of the light guide. Using the light guide for light sharing increases the light path length, and reduces light collection [19].

Finally, it is necessary to employ inexpensive photodetectors that are compact, pixellated, and have a fast rise time, low transit time jitter, and high quantum efficiency (QE) to improve time resolution [15]. As the fulfilling photosensors, Geiger-mode APDs (SSPM, SiPM, and MPPC) have been in the spotlight recently; G-APDs open up the possibility for multimodality to combine with MR systems because they are insensitive to magnetic fields [20-22] and have excellent timing properties.

Accordingly, in order to enhance the time performance in DOI detectors, it is necessary to improve the light collection efficiency, to reduce the path length of the scintillation light, and of course to use fast crystals with high light yield (i.e. LSO, LYSO, and $LaBr_3$) and fast photo-sensors with high QE and small transit time fluctuation referred to as time jitter. The DOI-encoding designs also should not cause too much light spread and it is desirable to use polished crystals (when using long crystals) in order to be suitable for TOF PET detectors.

DOI-ENCODING DESIGNS

For the foregoing purposes, various DOI-encoding designs have been proposed, as follows: 1) discrete DOI measurement by a multi-layer detector; 2) direct DOI measurement; 3) continuous DOI measurement by dual-ended; and 4) by single-ended readouts. The detector designs, concepts to extract DOI information, pros and cons, and the recent results are discussed in this section.

Discrete DOI measurement by multi-layer detectors

Multi-layer detectors consist of multiple layers of scintillation crystal arrays. There are several designs to distinguish the

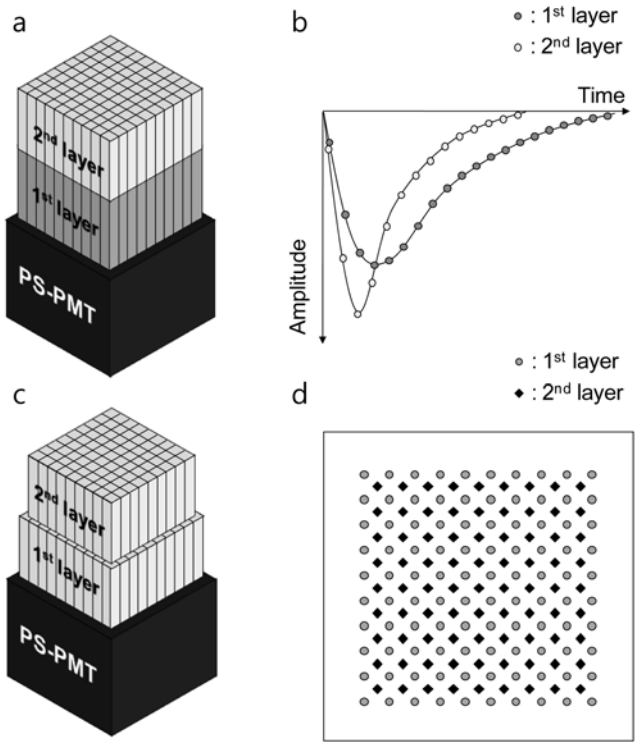

Fig. 2. Multi-layer DOI detector composed of the stacked two crystal layers and PS-PMT. (a) Schematic diagram of detector module using two kinds of crystals with different decay constants for pulse shape discrimination (PSD) method and (b) the output pulse shapes from individual layers. (c) Schematic diagram of detector module with a relative offset of the crystal layers and (d) the flood histogram pattern.

individual layers which interact with gamma rays, including: pulse-shape discrimination (PSD; the so-called "phoswich [phosphor sandwich"]; relative offset structure; and light-sharing method.

The PSD method employs a combination of several scintillation crystals with different decay time constants such as NaI(TI)/BGO and LSO/LuYAP [23, 24]. As an alternative to the use of different crystal materials, one kind of crystals with different concentrations of doping material was used as well.

In Fig. 2a, several different crystals were stacked on each other and optically-coupled to a common photo-sensor (PMT), and distinguished by different pulse-shape characteristics as shown in Fig. 2b. Various methods were proposed to quantify the differences in the pulse shape, as follows: constant fraction discrimination (CFD); rise time discrimination (RTD); constant time discrimination (CTD); charge comparison (CC); and delayed charge integration (DCI) methods [25-27]. Based on the comparison of the different PSD methods, the performance of those methods depends on the radiation detector and the signal-to-noise ratio [26]. The results of the PSD methods showed excellent layer identification with 1%~3% misidentification [28].

However, the multi-layer detectors provide discrete DOI information limited to the number of layers, and the DOI resolution is determined by the crystal length; the crystal length typically ranges from 5-10 mm [12]. Hence, this design has a trade-off relationship between the DOI resolution and the manufacturing cost because the number of crystals is related to the cost. Light collection loss occurs between layers. In fact, these disadvantages are common problems in multi-layer detector designs. In addition, PSD designs have a drawback in time performance due to different decay times [12].

The second approach illustrated in Fig. 2c is an offset structure with a dual-layer that has a relative offset of one-half a crystal pitch in both x- and y-directions [29, 30]. This approach was applied to three- and four-layer structures in combination with the PSD approach [31] and by relative shifting of all four layers to one-half a crystal pitch [32, 33]. In these designs, the DOI information can be estimated from the flood image (2D crystal position map), which is calculated by the centroid of light dispersion on a position-sensitive PMT (PS PMT). Because the centroid of light dispersion is shifted with the offset of crystal arrangement, the flood positions corresponding to crystals in all layers were separated in the flood image (Fig. 2d). This design requires one kind of crystal material, and has an advantage to reduce complications in electronics. However, an accurate arrangement is required not to overlap individual crystal flood peaks in the flood image. Regardless of how accurate the arrangement is placed, flood positions at the edge in the upper crystal layer are moved toward the center due to limited light dispersion at the edge of the crystal block [34], which causes overlapping of the flood positions and misidentification of crystals. This design has disadvantages in light collection and time performance due to light dispersion by the offset structure, and the above-mentioned common drawbacks for multi-layer detectors.

The light-sharing method in Fig. 3a utilizes different reflector arrangements in four layers [35, 36]. In the reflector arrangement, four crystals are covered together with a reflector while leaving the space between the four crystals uncovered as an air gap. Then, the flood positions of the four crystals are shifted toward the center of the array by the centroid shift of light distribution due to light sharing through the air gap between the four crystals. As shown in Fig. 3b, using the different arrangement of the reflectors, all crystals in four layers are distinguished in the flood image. This approach has been combined with the PSD method, and succeeded to apply to eight layers [37]. This approach has the same drawbacks as the offset structure. In the layer identification method using the flood image, the DOI accuracy is estimated by a peak-to-valley ratio in the flood profile images. As an increase in the number of layers, the

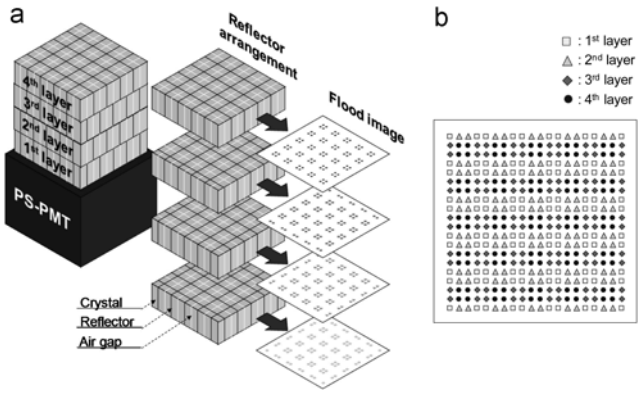

Fig. 3. Multi-layer DOI detector with light sharing method using different reflector arrangements. (a) Schematic diagram of the detector module, reflector arrangement and flood histogram pattern in each layer. (b) Flood histogram pattern (for 4-layer detector).

ratio becomes lower because of mis-positioning in the flood image by too much light dispersion and detector scattering events. Light-sharing structures increase the path length of the scintillation light, and cause light attenuation and deterioration in energy and time performance, resulting in a difference in peak values in energy distribution for individual layers that requires a very low threshold and application of different energy windows to select photoelectric events in individual layers.

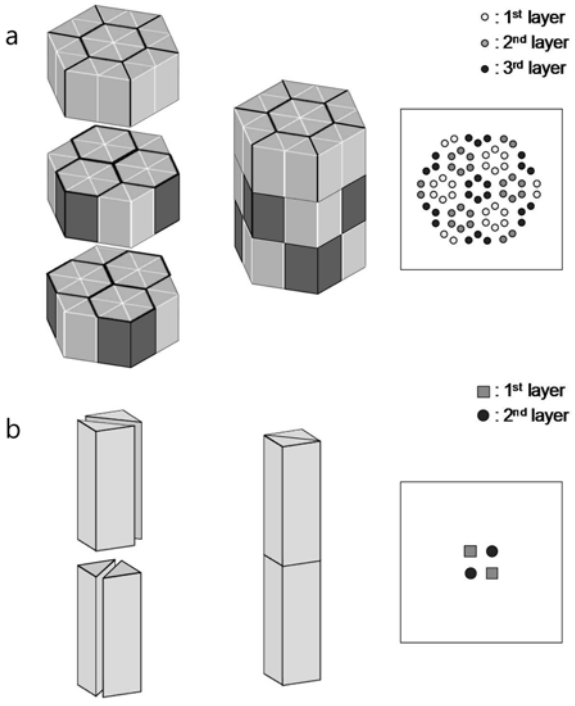

Fig. 4. Light sharing method using different reflector arrangements for triangular prisms. Schematic diagram of the detector module and the flood histogram patterns for (a) isosceles right (in horizontal cross section) triangle prisms in three layers and (b) equilateral triangle prisms in two layers.

This light sharing method was applied to two and three layers using unique crystals cut as triangular prisms, as follows: an equilateral triangle (in horizontal cross section) for two layers and an isosceles right triangle for three layers [38] in Figs. 4a and b. Those results showed that energy peak positions for individual layers are the same. In the two-layer constructed by 4 triangular prisms with isosceles right triangle cross sections (Fig. 4b), light dispersion is limited within the four crystals. Thus, it is expected that the two layer triangular prism design is attractive for TOF-DOI that has good energy and time performance providing DOI information.

Direct measurement of DOI positions

There are other approaches to directly obtain signals from individual depths. This approach consists of several layers of crystal arrays. The individual crystals were coupled to photosensors and the discrete DOI information is directly obtained by photosensers between crystal layers [39, 40].

An approach in Fig. 5a, originally proposed by Levin [41], was developed by the Standford group. A block detector is formed by stacking several module layers in which each layer consists of a small crystal array mounted on a PS-APD layer. The interacted crystal in the crystal array is identified by the flood image calculated four outputs signals per PS-APD. Because the large surface of small crystals is faced on the photosensor, this design has high light collection efficiency (>90%), and achieves excellent energy and time performances [42] because of the high light collection and the minimized light path length. Therefore, this design has advantages as a TOF-DOI detector. Readout of individual small crystals can distinguish detector scattering events as well. Currently, one detector unit consists of stacking 8 detector layers; one detector layer comprises two 8×8 LYSO crystal arrays with a crystal dimension of $0.91 \times 0.91 \times 1$ mm^3 coupled to two PS-APDs mounted on a flex circuit. Because of the crystal size, this detector has ~1 mm positioning resolution of gamma

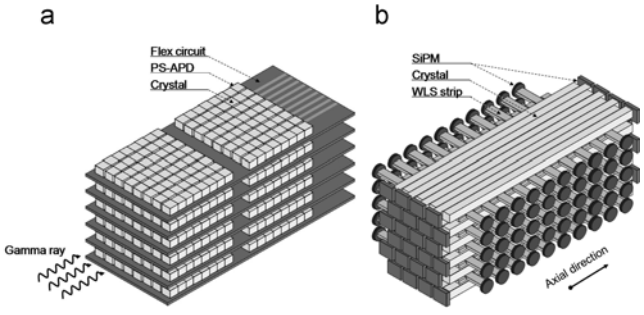

Fig. 5. Direct DOI-measuring detectors. (a) Stacked detector-layer module for directly measuring three-dimensional position of gamma ray interaction. (b) Axial PET detector module with axially arranged long scintillation crystals and WLS strips. The photosensors are G-APDs (SiPMs).

ray interaction in all directions. Using the two detector units, the coincidence point spread function (PSF) was obtained (average FWHM, 0.84 mm) and uniform across the arrays [42].

However, this technique requires very thin circuit boards and PS-APD elements to maintain a good packing fraction [12]. The manufacturing cost is also a problem because the cost rapidly increases with the great number of crystals, photosensors, and output channels.

The other design in Fig. 5b obtains depth-coordinate signals by orthogonally- stacked layers of thin WLS strips between the layers of the scintillation crystal array [43]. In this design, all signals were obtained from the ends of the individual crystals and WLS strips. The current structure of the detector module contains a 6×8 array of very long LYSO crystals ($3 \times 3 \times 100$ mm^3) and 6×26 WLS strips ($3 \times 0.9 \times 40$ mm^3) orthogonally-inserted on the top of each crystal layer; individual WLS strips were optically-isolated. G-APD photosensors (MPPCs) were optically-coupled to the ends of crystals and WLS strips. Based on the preliminary results obtained with the PMT trigger, it was expected that the detector module provides a positioning resolution of > 1.7 mm FWHM in the crystal-depth direction [44]. This design however involves the escalated cost by the increase of photosensor- and signal-densities as a common challenge for direct DOI measurements [12]. In contrast to the above-mentioned design developed by the Standford group, this approach using WLS is not suitable to combination with the TOF detector; time dispersion occurs due to measuring divided scintillation light by several photosensors, the difference of the transit distances between interaction position and individual photosensors, and the process to absorb and reemit light in WLS.

Continuous DOI measurement by dual-ended readout detectors

In this design, two photosensors are connected to both ends of a single crystal array, and measure light signals to compare the ratio between light outputs detected at one side and both sides. This approach, which was first proposed by Hamamatsu researchers [45], utilized two position-sensitive PMTs (Hamamatsu R2487) coupled to both ends of a 4×8 BGO ($3.75 \times 7 \times 100$ mm^3) crystal array. The DOI resolution was obtained to be approximately 9.5 mm FWHM for each irradiation positions at 10 mm intervals (100 mm length). In the full-ring system illustrated in Fig. 6, the long crystals were designed to be arranged in the axial direction. Thus, the axial spatial resolution of the system is dominated by the DOI resolution.

This design has also been developed by the UCLA, UC Davis, and CERN group using a 20-mm crystal array coupled to two APD arrays or PS-APDs, as illustrated in Fig. 7a [46-48]. Recently, this design was applied using SiPM arrays [49]. As the crystal length decreases to 20 mm, the DOI resolution was improved over the first design proposed by Hamamatsu researchers. The DOI accuracy depends on the crystal surface treatment and the size. The optimal surface and crystal size to achieve better DOI resolution was "as cut" rough surface and smaller surface (1.0×1.0 mm^2), respectively [46, 47]. Recent reports have shown that a DOI resolution of ~2 mm can be achieved using this approach with $1.0 \times 1.0 \times 20$ mm^3 rough (unpolished) crystals coupled to APDs [50].

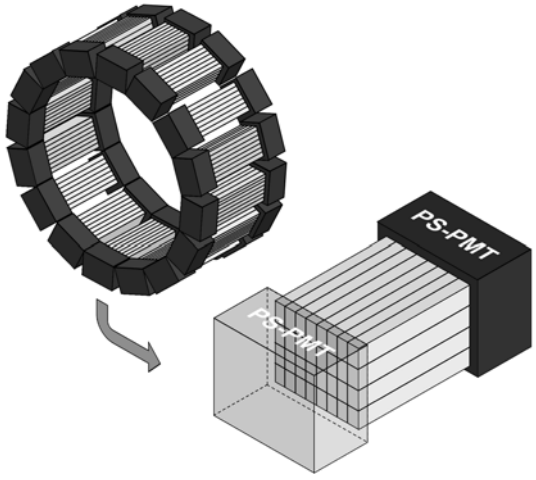

Fig. 6. Dual-ended readout detectors in which two PS-PMTs are coupled to both ends of a 4×8 crystal array.

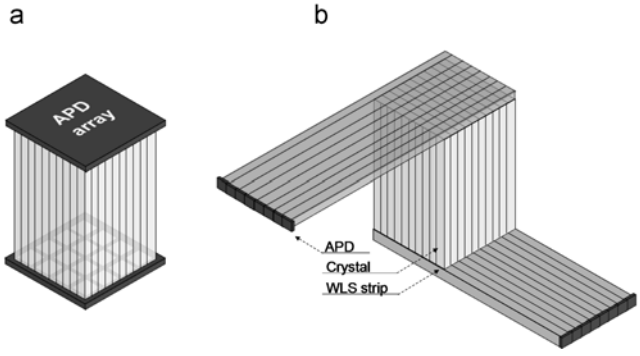

Fig. 7. Dual-ended readout detectors (a) using two APD arrays and (b) using WLS fibers orthogonally placed on the top and bottom of the scintillator array.

Compared with the multi-layer designs, this approach has an advantage to provide continuous DOI information with better DOI resolution. However, this design requires additional photo sensors. The increase (twice) in the number of photosensors leads the cost increase. In addition, compact ASIC front-end electronics are required to reduce the gamma ray attenuation and scattering by photosensors and electronics at the front of the crystal array. Radiation damage to solid-state photosensors and electronics by gamma rays is also a matter of concern, and the reduction of dead space between detector modules is

technically challenging [46].

There are several variations on this approach. One is the use of wavelength shifting (WLS) fibers, originally proposed by Worstell [51]. In Fig. 7b, the wavelength shifting (WLS) optical fibers are placed orthogonally on the top and botton of the scintillator array, and photosensors are coupled to one end of the WLS fibers for signal readout [52]. Since the WLS fibers readout the signals over row or column, that can reduce the number of photosensors. Accordingly, this approach is advantaged to build large-ring systems, and applied to develop a whole-body clinical PET/CT scanner, although the signals from WLS fibers at present are used to improve detector identification and energy resolution (compared with block detector design), rather than to acquire DOI information [51]. For acceptable performance, however, it is critical to maximize collection of light photons from the ends of the fibers and to minimize the optical crosstalk between adjacent fibers [52]. The use of optical fibers degrades time performance.

The other one is the use of monolithic crystal instead of a crystal array. This approach will be discussed in detail at the later section about monolithic crystal detectors.

Continuous DOI measurement by single-ended readout

The foregoing DOI-encoding designs require additional crystal arrays or additional photosensors that cause an increase in cost. Most of these DOI-encoding designs have not been translated into commercial systems due to the rapidly escalating cost [53]. More recently, there is some tendency for new DOI-encoding detectors to be designed with cost-effectiveness. Here, DOI-encoding designs for less cost are introduced.

Monolithic crystal detectors

General PET detectors consist of a crystal array (pixelated crystals) in which each crystal is optically isolated by reflector materials, whereas this monolithic crystal detector employs a continuous crystal slab (monolithic crystal block), as shown in Fig. 8a and b. Since this approach has no gap occupied by reflector materials, this one achieves high packing fraction. Making the crystal narrower for higher resolution causes more several problems, including inter-crystal scatter, light collection difficulty, practical difficulties of accurate and consistent crystal size [54]. In the continuous crystal, emitted scintillation light spreads until the optical photons are detected on the photosensors. The extent of light dispersion depends on the distance between the light-emitting position (DOI position or z position of interaction) and photosensor surface. The centroid of light dispersion is reflected in 2D position (x and y positions) of interaction. Accordingly, 3D interaction positions of gamma ray within the crystal slab are determined by measuring light distribution on a photo-sensor array (single-ended readout).

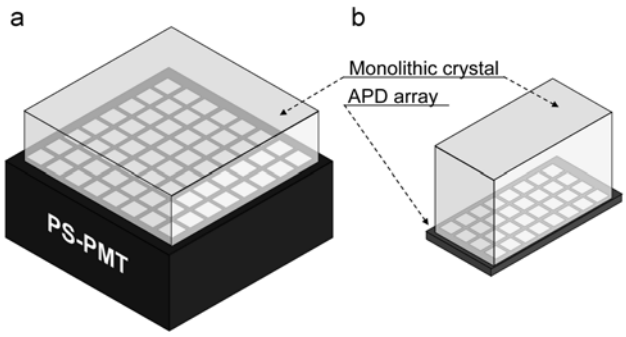

Fig. 8. Monolithic crystal detectors (a) using PS-PMT and (b) APD arrays.

However, using conventional Anger style positioning schemes, event positioning was distorted by edge effect artifacts (event overlap, spatial resolution degradation, and the FOV shrinkage at the edge) due to the restricted light spread at the crystal edges [55]. To improve position performance at the edge, rough surface treatment and black paint were required at the edge-side wall of the crystal. In addition to reduce the reflection at the edge of the crystal, a statistics-based (maximum likelihood) positioning algorithm has been implemented [55-57]. This algorithm relies upon characterizing the light response function (LRF) of each photosensor channel versus event location through Monte Carlo simulation, and estimates event positions according to the location that maximizes the likelihood function between the event data and the look-up table of the LRF [56].

To improve the performance of event positioning near the edges of a crystal slab, additional photosensors used to be placed at the edges of the crystal [55]. Currently, a detector module, developed by the University of Washington researchers, composed of a $50 \times 50 \times 8$ mm^3 crystal and a 64-anode PMT, provides a positioning resolution of a least 1.4 mm and 2 bits of DOI information [12]. However, the use of a thicker crystal to improve detection efficiency would still cause positional distortion near the edges of the crystal. The stacking of multiple slabs (monolithic crystal layers) has been proposed as a solution to this problem because this achieves high sensitivity, while maintaining good positional resolution within a slab [12].

The CERN group and Delft University of Technology researchers also have developed monolithic crystal detectors composed of a $20 \times 10 \times 10$ (depth) mm^3 crystal coupled to a 8×4 APD array. The positioning resolution of 1.5 mm FWHM and the DOI resolution of 1.8~3.0 mm were obtained in a 10-mm thick LSO block [58]. The detector module offered better performances when read out from the front-side than when read out from the back side because the majority of the annihilation gamma rays interact in the front one-half of the crystal [59]. In the case using two APD arrays coupled to both ends of the crystal, a 20-mm thick

monolithic crystal detector offers good spatial resolution similar to 10-mm thick crystals with single front read out [59]. This approach also employs PS-APDs or SiPMs as alternative sensors to APD arrays [60, 61].

Because the monolithic crystals have an advantage of collecting more light outputs and reduce path length of the scintillation light, it is anticipated that the monolithic crystal approach provides good timing performance with DOI information. Study of time walk correction by DOI information for the TOF PET detector was performed using a $20 \times 20 \times 12$ mm^3 LYSO crystal coupled to a fast 4×4 multi-anode PMT [62]. A coincidence timing resolution of 358 ps FWHM was obtained with a BaF_2 reference detector with a positioning resolution of 2.4 mm FWHM and a DOI resolution of 2.3 ~ 4 mm in a 12-mm thick crystal. However, the challenge is the ability to extract good event positioning near the edges of the crystal [12]. Maximum likelihood positioning has a high computational cost. Furthermore, it is extremely difficult to accurately model the light transport and detection in a scintillator detector and evaluate the accuracy compared with real data [56] because it is difficult to experimentally measure LRF at an accurately known source position over full space in the crystal; in a monolithic crystal, generating gamma ray interaction at a specific position is impossible. To solve the problem, a quasi-monolithic detector in Fig. 9a was proposed by the Yonsei University group. The design can obtain the LRF against event positions experimentally because the crystal elements are separated from each other in the axial direction and are monolithic in the trans-axial direction [63]. The experimentally-obtained LRF involves the effects of gain non-uniformity in PS-PMT, real detector geometry, and the parameter values that influence light transport and is difficult to accurately model in simulation.

The detector module composed of a 1D array of 8 LYSO crystals ($20 \times 2 \times 10$ mm^3) coupled to a 8×8 multi-anode PMT provides 2-mm positioning resolution (determined by crystal width) with 3 bits of DOI information (DOI positioning accuracy, 55%) [64]. However, it is still required to reduce the mispositioning rate in the DOI direction by increasing the number of LUT sampling points.

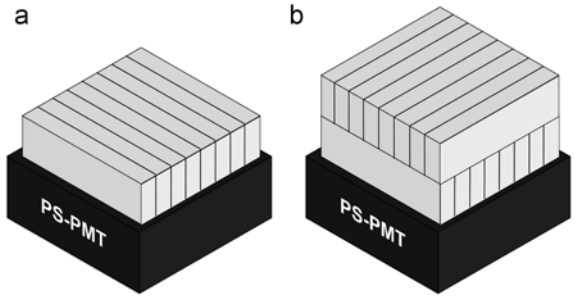

Fig. 9. (a) Quasi-monolithic crystal module and (b) cross-stack quasi-monolithic crystal module in two-layer configuration.

This design can be applied to a two-layer structure in which quasi-monolithic elements are stacked crosswise for high sensitivity, as illustrated in Fig. 9b [65]. In this two-layer cross-stack quasi-monolithic detector, LRF can be also obtained through experiments using the detector in which one quasi-monolithic crystal is a LYSO scintillator and the other crystals are dummies of silica or some materials that have a similar refractive index to the crystals.

Single crystal array + single-ended readout

There are several attempts to extract DOI information from a single crystal array using a single-ended readout because such detector structures are suitable to build a full-ring system with minimum gaps between detector blocks and have cost-effectiveness relative than to the multi-layer or dual-ended readout detector designs.

The first attempt (the dMiCE detector) proposed by Miyaoka and Lewellen was based on the coupled two crystals with triangular reflector between the two crystals packed together, as illustrated in Fig. 10a [66, 67]. Between the two crystals, the scintillation light can be shared because the crystals are partially covered by a triangular reflector, and the light sharing ratio reflects the DOI position. One-to-one coupling of individual crystals and compact photosensors is required to measure the exact light-sharing ratio. The DOI accuracy was improved by estimating the first event position of a multiple interaction within the crystal array using a statistical positioning algorithm [68]. The DOI resolution achieved to date using this approach is approximately 3-4 mm [12].

The second design in Fig. 10b is a phosphor-coated crystal detector in which the upper-half crystal surface is coated by the thin layer of the phosphor powder [27]. The phosphor absorbs scintillation light with a relatively short decay time, and re-emits "phosphor-converted" light with a longer decay time. Because the amount of scintillation light reaching the phosphor depends on the DOI position, the ratio of scintillation light and re-emitted phosphor-converted light is related to the DOI position. The light output signal contains both the lights with short and long decay times, and the shape of the output pulse is influenced by the ratio of the lights. Therefore, the DOI position can be determined by the shape of the output pulse. Although this approach utilizes the PSD method mentioned in the section of discrete DOI measurement (*vide supra*), it provides continuous DOI information. Using the delayed charge integration (DCI) method, the average DOI resolution (FWHM) obtained was 8.0 mm for $1.5 \times 1.5 \times 20$ mm^3 LSO crystals (4 x 4 array) half-coated with YGG phosphor [27]. The use of unpolished crystal is necessary in this approach, and causes large light collection loss along the DOI position, so that the photoelectric-peak position in the energy spectrum decreases with an

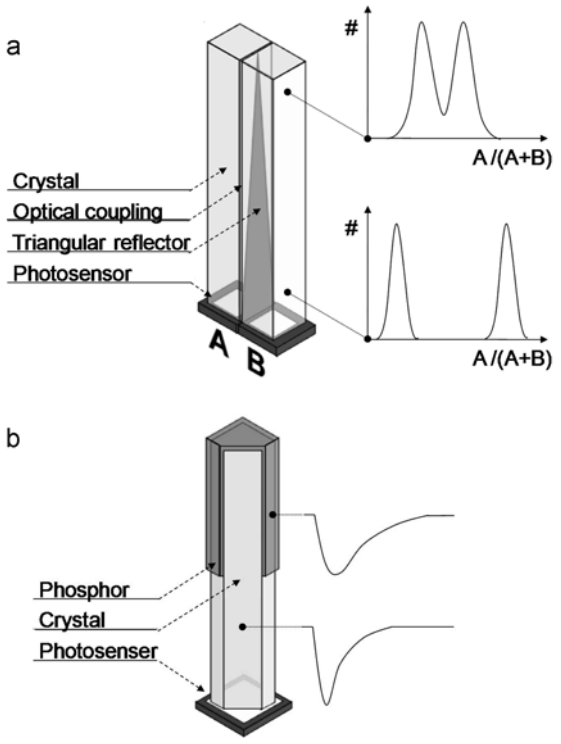

Fig. 10. Single-ended readout detectors for continuous-DOI measurement. (a) cMiCE detector using the coupled two crystals with triangular reflector between the crystals. (b) phosphor-coated crystal detector in which the phosphor absorbs and re-emits the scintillation light.

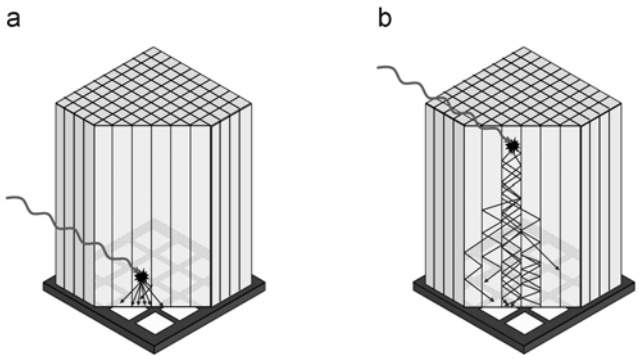

Fig. 11. Single-ended readout detector for continuous-DOI measurement using scintillation light cross-talks. Light dispersion through reflectors when the gamma ray interaction occurs (a) nearby and (b) far away from the photosensors.

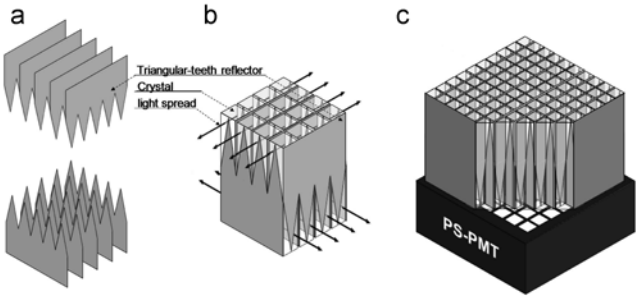

Fig. 12. Single-ended readout detector for continuous-DOI measurement using 2D light spread tailored by geometric shape of reflector strips. (a) Crossing triangular-teeth strips for reflector frame. (b) 2D light dispersion around the reflector teeth within a crystal array. (c) Detector module composed of a single crystal array and single-ended readout.

increase in the distance between the DOI position and PMT surface [27]. Lower light collection leads to poorer flood histograms and timing performances.

The other design is the way to examine the DOI-dependent light spread due to optical crosstalk between crystal elements on the sensitive pixel array in multi-channel PMT. Although the individual crystals are covered by reflectors, leakage of scintillation light in Fig. 11 occurs across the partially transparent reflector barrier between the crystals, and depends on the DOI positions [69]. This approach requires "as cut" rough surface of crystals as well. Thus, light collection loss occurs along the DOI positions. The DOI resolution of 8 mm was obtained using "as cut" rough crystals [69].

This approach has cost-effectiveness and advantage to easily identify the crystal positions and improve spatial resolution by using smaller crystals. However, a challenge for these detectors is to improve DOI resolution as well as the dual-ended readout detector design. It is difficult to tailor DOI dependency using scintillation light within the pixelated crystal array and improve DOI resolution.

In order to improve DOI resolution, our group at Seoul National University has proposed a novel DOI-encoding design in which 2D DOI-dependent light dispersion was tailored by the geometric shape of reflectors around crystals (triangular-teeth strip in Fig. 12a) [70]. This 2D light dispersion can increase the contrast of DOI dependency along the DOI position than the 1D light dispersion. As shown in Fig. 12b, crystals are partially covered by reflectors because of the triangular teeth shape. Scintillation light can spread through the uncovered area around the triangular-teeth reflectors. Then, the directions of the spreading light via reflectors are different between the upper and lower half of the crystal array because the reflector strips cross over each other and reverse direction to make a matrix frame. In addition, the extent of light dispersion depends on the DOI positions due to the different width of the uncovered area along the DOI positions. Therefore, this 2D light-sharing method allowed better DOI resolution to be obtained for very long crystals. This design requires the crystal surface to be unpolished (rough surface, "as cut") in order to cause light dispersion within a crystal array. We have experimentally-obtained a DOI resolution of 3.5 mm at the center of the rough and very long LYSO crystal array ($2 \times 2 \times 28$ mm^3) coupled to an 8×8 multi-anode PMT in Fig. 12c. The devised design provides

better DOI information with cost-effectiveness and clear crystal identification using a flood image.

However, since all these designs for continuous DOI measurement rely upon using rough surface crystals to tailor DOI dependency using scintillation light, the rough surface increases the light path length and causes light absorption within the crystals. Then, the light collection efficiency becomes rapidly decreased with increasing distance between the DOI position and photosensors. The light collection loss along the DOI position brings degradation of time performance in the detectors. To improve time performance, these designs should have high and uniform light collection efficiency against the DOI position, thus it is desirable to extract DOI information within a polished crystal array.

DISCUSSION

Most DOI-encoding approaches have a tradeoff relationship between DOI resolution and other performances. So far, there has been still no design to perfectly satisfy the requirements. Although the conventional DOI-encoding approaches were designed without consideration of time performance, new approaches with high-time resolution are now required. Because the factors to improve time performance (high light collection, fast photosensors with high QE, and one-to-one coupling of crystal and photosensor) also enhance the other performances in PET, the combined DOI-TOF technique will be actively investigated.

As an increasing awareness to reduce injected dose, the importance of improving sensitivity will be magnified. Then, the DOI-encoding technique helps building smaller ring systems close to the patient for high sensitivity, while providing a large FOV in the future.

There is an optional requirement in DOI-encoding designs involving the ability to distinguish the first interaction position for multiple scattering (inter-detector scatter) within a detector. In most scintillation crystals used in PET, the probability of a photoelectric interaction (total absorption) on the first interaction is < 50% for 511 keV gamma rays (BGO, 43%; LSO, 34%; and NaI(TI), 18%) [12]. Then, a thicker crystal detector for high sensitivity increases inter-detector scatter events. The ratio of inter-detector scatter has been reported to reach 40% against total measured events for thick crystal block (total dimension of the crystal block is $48 \times 48 \times 30$ mm^3), and 34% of the inter-detector scatters remains after energy cut [71]. Because the inter-detector scatter degrades crystal identification and DOI accuracy, it can be expected that the inter-detector scatter leads the spatial resolution loss of the detector module. To eliminate the artifact due to the detector scatter, algorithms to find the first interaction position in multiple interactions (detector scatter) were investigated [72, 73]. However, the study based on Monte Carlo simulation indicated that detector scatter may have a small effect (6%~8%) on the image resolution (FWHM) of a reconstructed point source for the DOI capable detector systems [74-76]. Despite the small improvement, finding the first interaction position requires processing additional large amounts of data; with only TOF and DOI information, the TOF-DOI scanner already has a high computational cost for reconstruction.

However, although the deterioration of resolution (FWHM) by detector scatter effect is small, considerable noise and contrast loss in the image are caused by the tails of coincidence line response function resulting from the detector scatter [75]. Therefore, the need of identifying the first interaction position in the detector scatter may depend on the optimal level between improvement of image quality and the progress of the computational speed.

ACKNOWLEDGMENTS

This work was supported by grants from the Atomic Energy R&D Program (2008-2003852, and 2010-0026012) through the Korea Science and Engineering Foundation funded by the Korean Ministry of Education, Science and Technology, and SNU-KAERI Degree & Research center for Radiation Convergence Sciences from the Korea Research Council of Foundation Science and Technology.

REFERENCES

[1] Price P. PET as a potential tool for imaging molecular mechanisms of oncology in man. Trends Mol Med. 2001; 7(10):442-26.
[2] Jagoda EM, Vaquero JJ, Seidel J, Green MV, Eckelman WC. Experiment assessment of mass effects in the rat: implications for small animal PET imaging. Nucl Med Biol. 2004; 31(6):771-9.
[3] Derenzo SE, Moses WW, Jackson HG, Turko BT, Cahoon JL, Geyer AB, Vuletich T. Initial characterization of a position-sensitive photodiode/BGO detector for PET. IEEE T Nucl Sci. 1989; 36(1):1084-9.
[4] Moses WW. Trends in PET imaging. Nucl Instrum Meth A. 2001; 471:209-14.
[5] Kim JS, Lee JS, Im KC, Kim SJ, Kim SY, Lee DS, Moon DH. Performance measurement of the microPET Focus 120 scanner. J Nucl Med. 2007; 48(9):1527-35.
[6] Visser EP, Disselhorst JA, Brom M, Laverman P, Gotthardt M, Oyen WJ, Boerman OC. Spatial resolution and sensitivity of the Inveon small-animal PET scanner. J Nucl Med. 2009; 50(1):139-47.
[7] MacDonald LR, Dahlbom M. Parallax correction in PET using depth of interaction information. IEEE T Nucl Sci. 1998; 45(4):2232-7.
[8] Lee JS. Technical advances in current PET and hybrid imaging systems. Open Nucl Med J. 2010; 2:192-208.
[9] Shibuya K, Nishikido F, Inadama N, Yoshida E, Chihfung Lam, Tsuda T, Yamaya T, Murayama H. Timing resolution improved by DOI information in an LYSO TOF-PET detector. Conf Rec

IEEE NSS MIC. 2007; M19-7.
[10] Spanoudaki VCh, Levin CS. Investigating the temporal resolution limits of scintillation detection from pixelated elements: comparison between experiment and simulation. Phys Med Biol. 2011; 56(3):735-56.
[11] Surti S, Karp JS. Design considerations for a limited angle, dedicated breast, TOF PET scanner. Phys Med Biol. 2008; 53(11):2911-21.
[12] Lewellen TK. Recent developments in PET detector technology. Phys Med Biol. 2008; 53:R287-317.
[13] Liu S, Li H, Zhang Y, Ramirez RA, Baghaei H, An S, Wang C, Liu J, Wong WH. Monte Carlo simulation study on the time resolution of a PMT-quadrant-sharing LSO detector block for time-of-flight PET. IEEE T Nucl Sci. 2009; 56(5):2614-20.
[14] Moses WW, Derenzo SE. Prospects for time-of-flight PET using LSO scintillator. IEEE T Nucl Sci. 1999; 46(3):474-7.
[15] Moses WW. Recent advances and future advances in time-of-flight PET. Nucl Instrum Meth A. 2007; 580(2):919-24.
[16] Xiaobuang Y. A study of light collection efficiency in scintillation detectors. Nucl Instrum Meth A. 1984; 228(1):101-4.
[17] Aykac M, Bauer F, Williams CW, Loope M, Schmand M. Recent timing performance of Hi-Rez detector for time-of-flight (TOF) PET. IEEE T Nucl Sci. 2008; 53(3):1084-9.
[18] Moisan C, Vozza D, Loope M. Simulating the performances of an LSO based position encoding detector for PET. IEEE T Nucl Sci. 1997; 44(6):2450-8.
[19] Moszynski M, Kapusta M, Nassalski A, Szczesniak T, Wolski D, Eriksson L, Melcher CL. New prospects for time-of-flight PET with LSO scintillator. IEEE T Nucl Sci. 2006; 53(5):2484-8.
[20] Hong SJ, Song IC, Ito M, Kwon SI, Lee GS, Sim KS, Park KS, Rhee JT, Lee JS. An investigation into the use of Geiger-mode solide-state photomultipliers for simultaneous PET and MRI acquisition. IEEE T Nucl Sci. 2008; 55(3):882-8.
[21] Lee JS, Hong SJ. Geiger-mode avalanche photodiodes for PET/MRI. In: Iniewski K, editor. Electronic circuits for radiation detection. Boca Raton: CRC Press LLC; 2010. pp. 179-200.
[22] Kwon SI, Lee JS, Yoon HS, Ito M, Ko GB, Choi JY, Lee SH, Chan Song I, Jeong JM, Lee DS, Hong SJ. Development of small-animal PET prototype using silicon photomultiplier (SiPM): initial results of phantom and animal imaging studies. J Nucl Med. 2011; 52(4):572-9.
[23] Karp JS, Daube-Withespoon ME. Depth-of-interaction determination in NaI(TI) and BGO scintillation crystals using a temperature gradient. Nucl Instrum Meth A. 1987; 260:509-17.
[24] Jung JH, Choi Y, Chung YH, Devroede O, Krieguer M. Bruyndonckx P, Tavernier S. Optimization of LSO/LuYAP phoswich detector for small animal PET. Nucl Instrum Meth A. 2007; 571:669-75.
[25] Seidel J, Vaquero JJ, Siegel S, Gandler WR, Green MV. Depth identification accuracy of a three layer phoswich PET detector module. IEEE T Nucl Sci. 1999; 46(3):485-90.
[26] Chandrikamohan P, DeVol TA. Comparison of pulse shape discrimination methods for phoswich and CsI:Tl detectors. IEEE T Nucl Sci. 2007; 54(2):398-403.
[27] Du H, Yang Y, Glodo J, Wu Y, Shah K, Cherry SR. Continuous depth-of-interaction encoding using phosphor-coated scintillators. Phys Med Biol. 2009; 54(6):1757-71.
[28] Streun M, Brandenburg G, Larue H, Saleh H, Zimmermann E, Ziemons K, Halling H. Pulse shape discrimination of LSO and LuYAP scintillators for depth of interaction detection in PET. IEEE T Nucl Sci. 2003; 50(3):344-7.
[29] Liu H, Omura T, Watanabe M, Yamashita T. Development of a depth of interaction detector for gamma-rays. Nucl Instrum Meth A. 2001; 459:182-90.
[30] Zhang N, Thompson CJ, Togane D, Cayouette F, Nguyen KQ. Anode position and last dynode timing circuits for dual-layer BGO scintillator with PS-PMT based modular PET detectors. IEEE T Nucl Sci. 2002; 49(5):2203-7.
[31] Hong SJ, Kwon SI, Ito M, Lee GS, Sim KS, Park KS, Rhee JT, Lee JS. Concept verification of three-layer DOI detectors for animal PET. IEEE T Nucl Sci. 2008; 55(3):912-7.
[32] Ito M, Lee JS, Kwon SI, Lee GS, Hong B, Lee KS, Sim KS, Lee SJ, Rhee JT, Hong SJ. A four-layer DOI detector with a relative offset for use in an animal PET system. IEEE T Nucl Sci. 2010; 57(3):976-82.
[33] Chung YH, Hwang JH, Baek C-H, Lee S-J, Ito M, Lee JS, Hong SJ. Monte Carlo simulation of a four-layer DOI detector with relative offset in animal PET. Nucl Instrum Meth A. 2011; 626-7:43-50.
[34] Ito M, Hong SJ, Lee JS, Kwon SI, Lee GS, Park KS, Hong B, Lee KS, Lee SJ, Rhee JT, Sim KS. Four-layer DOI detector with a relative offset in animal PET system. Conf Rec IEEE NSS MIC. 2007; M26-76.
[35] Murayama H, Ishibashi I, Uchida H, Omura T, Yamashita T. Depth encoding multicrystal detectors for PET. IEEE T Nucl Sci. 1998; 45(3):1152-8.
[36] Tsuda T, Murayama H, Kitamura K, Yamaya T, Yoshida E, Omura T, Kawai H, Inadama N, Orita N. A four-layer depth of interaction detector block for small animal PET. IEEE T Nucl Sci. 2004; 51(5):2537-42.
[37] Inadama N, Murayama H, Hamamoto M, Tsuda T, Ono Y, Yamaya T, Yoshida E, Shibuya K, Nishikido F. 8-layer DOI encoding of 3-dimensional crystal array. Conf Rec IEEE NSS MIC. 2005; J01-5.
[38] Inadama N, Murayama H, Yamaya T, Nishikido F, Shibuya K, Yoshida E, Tsuda T, Ohmura A, Yazaki Y, Osada H. DOI PET detectors with scintillation crystals cut as triangular prisms. Conf Rec IEEE NSS MIC. 2008; M06-201.
[39] Rafecas M, Boning G, Pichler BJ, Lorenz E, Schwaiger M, Ziegler SI. A Monte Carlo study of high-resolution PET with Granulated dual-layer detectors. IEEE T Nucl Sci. 2001; 48(4):1490-5.
[40] McElroy DP, Hoose M, Pimpl W, Spanoudaki V, Schüler T, Ziegler SI. A true singles list-mode data acquisition system for a small animal PET scanner with independent crystal readout. Phys Med Biol. 2005; 50(14):3323-35.
[41] Levin CS. Design of a high-resolution and high-sensitivity scintillation crystal array for PET with nearly complete light collection. IEEE T Nucl Sci. 2000; 49(5):2236-43.
[42] Vandenbroucke A, Foudray AM, Olcott PD, Levin CS. Performance characterization of a new high resolution PET scintillation detector. Phys Med Biol. 2010; 55(19):5895-911.
[43] Braem A, Chesi E, Joram C, Séguinot J, Weilhammer P, De Leo R, Nappi E, Lustermann W, Schinzel D, Johnson I, Renker D, Albrecht S. High precision axial coordinate readout for an axial 3-D PET detector module using a wavelength shifter strip matrix. Nucl Instrum Meth A. 2007; 580(3):1513-21.
[44] Beltrame P, Bolle E, Braem A, Casella C, Chesi E, Clinthorne N, Cochran E, De Leo R, Dissertori G, Djambazov G, Fanti V, Honscheid K, Huh S, Johnson I, Joram C, Kagan H, Lustermann W, Meddi F, Nappi E, Nessi-Tedaldi F, Oliver JF, Pauss P, Rafecas M, Renker D, Rudge A, Schinzel D, Schneider T, Seguinot J, Smith S, Solevi P, Stapnes S, Weilhammer P. Construction and tests of demonstrator modules for a 3-D axial PET system for brain or small animal imaging. Nucl Instrum Meth A. [In press].
[45] Shimizu K, Ohmura T, Watanabe M, Uchida H, Yamashita T. Development of 3-D detector system for positron CT. IEEE T Nucl Sci. 1988; 35(1):717-21.
[46] Shao Y, Silverman RW, Farrell R, Cirignano L, Grazioso R, Shah KS, Vissel G, Clajus M, Tumer TO, Cherry SR. Design studies of a high resolution PET detector using APD arrays.

IEEE T Nucl Sci. 2000; 47(3):1051-7.
[47] Yang Y, Dokhale PA, Silverman RW, Shah KS, McClish MA, Farrell R, Entine G, Cherry SR. Depth of interaction resolution measurements for a high resolution PET detector using position sensitive avalanche photodiodes. Phys Med Biol. 2006; 51(9):2131-42.
[48] Abreu MC, Aguiar JD, Almeida FG, Almeida P, Bento P, Carrico B, Ferreira M, Ferreira NC, Goncalves F, Leong C, Lopes F, Lousa P, Martins MV, Matela N, Mendes PR, Moura R, Nobre J, Oliveira N, Ortigao C, Peralta L, Pereira R, Rego J, Ribeiro R, Rodrigues P, Sampaio J, Santos AI, Silva L, Silva JC, Sousa P, Teixeira IC, Teixeira JP, Trindade A, Varela J. Design and evaluation of the Clear-PEM scanner for positron emission mammography. IEEE T Nucl Sci. 2006; 53(1):71-7.
[49] Shao Y, Li H, Gao K. Initial experimental studies of using solid-state photomultiplier for PET applications. Nucl Instrum Meth A. 2007; 580(2):944-50.
[50] Yang Y, Wu Y, Qi J, James SS, Du H, Dokhale PA, Shah KS, Farrell R, Cherry SR. A prototype PET scanner with DOI-encoding detectors. J Nucl Med. 2008; 49(7):1132-40.
[51] Worstell W, Adler S, Domigan P, Johnson O, Kudrolli H, Lazuka D, Monteverde P, Nevin J, Rohatgi R, Romanov L, Starsja S. Design and performance of a prototype whole-body PET/CT scanner with fiber optic readout. Conf Rec IEEE NSS MIC. 2004; 3280-4.
[52] Du H, Yang Y, Cherry SR. Measurements of wavelength shifting (WLS) fibre readout for a highly multiplexed, depth-encoding PET detector. Phys Med Biol. 2007; 52(9):2499-514.
[53] Lewellen TK. The challenge of detector designs for PET. AJR Am J Roentgenol. 2010; 195(2):301-9.
[54] Cherry SR, Shao Y, Tornai MP, Siegel S, Ricci AR, Phelps ME. Collection of scintillation light from small BGO crystals. IEEE T Nucl Sci. 1995; 42(4):1058-63.
[55] Joung J, Miyaoka RS, Lewellen TK. cMiCE: a high resolution animal PET using continuous LSO with a statistics based positioning scheme. Nucl Instrum Meth A. 2002; 489(1-3):584-98.
[56] Ling T, Lewellen TK, Miyaoka RS. Depth of interaction decoding of a continuous crystal detector module. Phys Med Biol. 2007; 52(8):2213-28.
[57] van der Laan DJ, Maas MC, Schaart DR, Bruyndonckx P, Lamaitre C, van Eijk CWE. Spatial resolution in positionsensitive monolithic scintillation detectors. Conf Rec IEEE NSS MIC. 2006; 2506-10.
[58] Bruyndonckx P, Leonard S, Liu J, Tavernier S, Szupryczynski P, Fedorov A. Study of spatial resolution and depth of interaction of APD-based PET detector modules using light sharing schemes. IEEE T Nucl Sci. 2003; 50(5):1415-19.
[59] Maas MC, van der Laan DJ, Schaart DR, Huizenga J, Brouwer JC, Bruyndonckx P, Leonard S, Lemaitre C, van Eijk CWE. Experimental characterization of monolithic-crystal small animal PET detectors read out by APD arrays. IEEE T Nucl Sci. 2006; 53(3):1071-7.
[60] Bruyndonckx P, Lemaître C, Schaart D, Maas M, van der Laan DJ, Krieguer M, Devroede O, Tavernier S. Towards a continuous crystal APD-based PET detector design. Nucl Instrum Meth A. 2007; 571(1-2):182-6.
[61] Schaart DR, van Dam HT, Seifert S, Vinke R, Dendooven P, Löhner H, Beekman FJ. A novel, SiPM-array-based, monolithic scintillator detector for PET. Phys Med Biol. 2009; 54(11):3501-12.
[62] Vinke R, Löhner H, Schaart DR, van Dam HT, Seifert S, Beekman FJ, Dendooven P. Time walk correction for TOF-PET detectors based on a monolithic scintillation crystal coupled to a photosensor array. Nucl Instrum Meth A. 2010; 621(1-3):595-604.
[63] Chung YH, Lee S-J, Beak C-H, Choi Y. New design of a quasimonolithic detector module with DOI capability for small animal PET. Nucl Instrum Meth A. 2008; 593(3):588-91.
[64] Lee S-J, Baek C-H, Hwang JY, Choi Y, Chung YH. Preliminary experimental results of a quasi-monolithic detector with DOI capability for a small animal PET. Nucl Instrum Meth A. 2010; 621:590-4.
[65] Lee S-J, Baek C-H, Chung YH, Choi Y. A cross-stack quasimonolithic detector with DOI capability for a small animal PET. Conf Rec IEEE NSS MIC, 2008; M06-81.
[66] Miyaoka RS, Lewellen TK. Design of a depth of interaction (DOI) PET detector module. IEEE T Nucl Sci. 1998; 45(4):1069-73.
[67] Lewellen TK, Janes M, Miyaoka RS. DMice-a depth-of-interaction detector design for PET scanners. Conf Rec IEEE NSS MIC. 2002; 2288-92.
[68] Champley KM, Lewellen TK, MacDonald LR, Miyaoka RS, Kinahan PE. Statistical three-dimensional positioning algorithm for high-resolution dMiCE PET detector. Conf Rec IEEE NSS MIC. 2008; 4751-4.
[69] Yang Y, Wu Y, Cherry SR. Investigation of depth of interaction encoding for a pixelated LSO array with a single multi-channel PMT. IEEE T Nucl Sci. 2009; 56(5):2594-9.
[70] Ito M, Lee JS, Park MJ, Sim KS, Hong SJ. Design and simulation of a novel method for determining depth-of-interaction in a PET scintillation crystal array using a single-ended readout by a multi-anode PMT. Phys Med Biol. 2010; 55(13):3827-41.
[71] Haneishi H, Sato M, Inadama N, Murayama H. Simplified simulation of four-layer depth of interaction detector for PET. Radiol Phys Technol. 2008; 1(1):106-14.
[72] Cho ZH, Juh SC. Resolution and sensitivity improvement in positron emission tomography by the first interaction point determination. Conf Rec IEEE NSS MIC. 1991; 1623-7.
[73] Comanor KA, Virador PRG, Moses WW. Algorithms to identify detector Compton scatter in PET modules. IEEE T Nucl Sci. 1996; 43(4):2213-9.
[74] Miyaoka RS, Lewellen TK. Effect of detector scatter on the decoding accuracy of a DOI detector. IEEE T Nucl Sci. 2000; 47(4):1614-9.
[75] Park S-J, Rogers WL, Clinthorne NH. Effect of inter-crystal Compton scatter on efficiency and image noise in small animal PET module. Conf Rec IEEE NSS MIC. 2003; M3-115.
[76] Lashkari S, Sarkar S, Ay MR, Rahmim A. The influence of crystal material on intercrystal scattering and the parallax effect in PET block detectors: A Monte Carlo study. IFMBE Proc. 2008; 21(8):633-6.